JOURNAL OF SOLID STATE CHEMISTRY 137, 325–331 (1998)
ARTICLE NO. SC987743

Surface Coordinate Geometry of Iron Catalysts: Formation of Tetrahedral/Octahedral Site on Silica Surface with/without Sodium Promoter

Hui Zhang,* Jiang-zhong Niu,* Yuan Kou,*,[1] Tsunehiro Tanaka,† and Satohiro Yoshida†

*Lanzhou Institute of Chemical Physics, Chinese Academy of Sciences, Lanzhou 730000, China; and †Department of Molecular Engineering, Kyoto University, Kyoto 606-01, Japan

Received September 9, 1997; in revised form December 24, 1997; accepted January 1, 1998

Sodium-modified, silica-supported iron oxide catalysts ($Na–Fe/SiO_2$) calcined at 300, 500, 650, and 800°C have been compared with unmodified Fe/SiO_2 treated in the same conditions by using Fe *K*-edge XANES, EXAFS, XRD, and Mössbauer techniques. Each iron on Fe/SiO_2 is found to have 5.0 nearest oxygen neighbors at an average distance of 1.94 Å; there is no change after calcination at 800°C. However, remarkable changes have been observed for $Na–Fe/SiO_2$ calcined at temperatures higher than 500°C. After calcination at 800°C, only tetrahedrally coordinated Fe^{3+} is observed. Accordingly, the coordination number of the nearest oxygens decreases to 4.1 with a significantly shortened Fe–O bond length of 1.89 Å. Supporting irons on sodium-pretreated silica ($Fe/Na–SiO_2$) and then calcinating the catalyst obtained at 800°C results in a similar phenomenon. © 1998 Academic Press

Key Words: **iron catalyst, silica-supported, sodium-promoted, site-symmetry, octahedral to tetrahedral, XANES, EXAFS, Mössbauer**

1. INTRODUCTION

The influence of the surface site-symmetry of a supported metal oxide on its catalytic behavior has not received enough attention (1–6). Many metal oxides are believed to undergo reconstruction after being supported on an oxide surface and then under catalytic reaction conditions, but lack of a suitable technique to examine the surfaces directly usually limits the observation. In this aspect, XAFS (X-ray absorption fine structure) is perhaps the most usable tool to touch the problem. 3D metals in compounds and complexes usually exhibit several very distinct features in their *K*-edge X-ray absorption near edge structure (XANES). The features, including the relative intensities of the pre-edge peaks, the energy positions of the E_0, and the absorption maximum, are sensitive to the local geometry of a central absorbing atom and vary with the change in its coordination. Furthermore, EXAFS (extended XAFS) can provide a more detailed description of the coordination surrounding the central atom in an average sense. By means of this technique, we have recently demonstrated that coordinately unsaturated octahedral cationic iron sites are of particular importance in the hydrogenation of CO (7) and CO_2 (8, 9). It is reasonable to question what will happen when the site-symmetry changes to tetrahedral.

Preparation of a predominantly tetrahedral phase for a desired element on an oxide surface has not been reported. This work is therefore carried out and finds that a predominant tetrahedral iron oxide phase can be easily obtained on silica surface by pretreatment of a sodium promoter and then calcination at a higher temperature. The changes in iron site-geometries under different pretreatment conditions have been extensively investigated in this paper using Fe *K*-edge XANES and EXAFS. Although the influences of a sodium promoter on the surface structure and the catalytic behavior of a catalyst so obtained have been widely investigated (10–13), this is the first work to report that the surface site-symmetry of supported iron oxides may change from octahedral to tetrahedral through participation of a sodium species.

2. EXPERIMENTAL

Fe/SiO_2 was prepared by incipient wetness impregnation with an aqueous solution of $Fe(NO_3)_3 \cdot 9H_2O$ (2). The sodium-modified $Na–Fe/SiO_2$ was prepared by coimpregnation with an aqueous solution of $Fe(NO_3) \cdot 9H_2O$ and $NaNO_3$. The samples obtained were dried at 120°C and then calcined at 300, 500, 650, and 800°C for 4 h. Sodium-pretreated silica ($Na–SiO_2$) was prepared by incipient wetness impregnation with an aqueous solution of $NaNO_3$. The samples obtained were dried at 120°C and then calcined

[1]To whom correspondence should be addressed. Present address: College of Chemistry and Molecular Engineering, Peking University, Beijing 100871, China.

0022-4596/98 $25.00

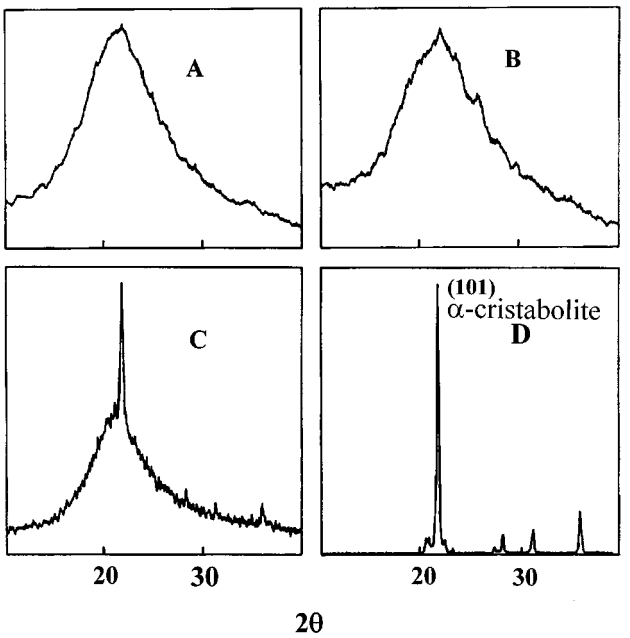

FIG. 1. X-ray diffraction pattern of (a) SiO_2 after calcination at 800°C, (b) Fe/SiO_2 after calcination at 800°C, (c) $Fe/Na–SiO_2$–I (simply dried at 120°C), and (d) $Fe/Na–SiO_2$–II (recalcined at 800°C).

at 650 and 800°C for 4 h. XRD patterns shown in Fig. 1c clearly indicate that in the presence of a sodium promoter the amorphous SiO_2 changes to α-cristobalite by heating to above 650°C (12). The resulting $Na–SiO_2$ was used as support to prepare $Fe/Na–SiO_2$ by the same method as that of Fe/SiO_2. One of the $Fe/Na–SiO_2$ samples obtained from the $Na–SiO_2$ calcined at 650°C (named $Fe/Na–SiO_2$–I) was dried at 120°C without recalcination. The sample from $Na–SiO_2$ calcined at 800°C (named $Fe/Na–SiO_2$–II) was dried at 120°C and then recalcined at 800°C. The loadings of iron and sodium were all 1 wt.%.

A D/MAX-RB X-ray diffractometer (Rigaku, Japan) operating with Cu$K\alpha$ radiation was used to determine the crystalline phase present. The XRD patterns of (a) commercial silica calcined at 800°C, (b) Fe/SiO_2 calcined at 800°C, (c) $Fe/Na–SiO_2$–I, and (d) $Fe/Na–SiO_2$–II are shown in Fig. 1.

All ^{57}Fe–Mössbauer spectra were taken at room temperature in an MR-351 Mössbauer spectrometer. The γ-ray source consisted of 10 mCi of Co in a rhodium matrix. The oscillation was in constant acceleration mode.

X-ray absorption spectra were obtained using the BL-7C facilities at the Photon Factory (Tsukuba, Japan) with a positron beam energy of 2.5 GeV and an average stored current of 250 mA. Data were recorded with an Si(111) double-crystal monochromater in transmission mode for pure compounds and in fluorescence mode for supported samples. The signal was integrated for 4 s at each point. The energy calibration was set as 7111.0 eV at the Fe edge. The data was collected in steps of 0.5 eV in the edge region. The samples maintained under nitrogen were sealed in flasks for performing the XAS measurement. The finely powdered specimens were applied directly to Scotch tape and then immediately measured at ambient temperature.

XANES data were normalized within 70 eV (−20 to 50 eV) about the edge. The absorption threshold E_T used as the zero of energy was taken with respect to the first inflection point, while the routine E_0 was taken at the maximum in the derivative spectrum. EXAFS data were processed using the Program for EXAFS data analysis written by the Institute of Physics, Chinese Academy of Sciences. This allows the EXAFS data to be extracted after pre- and post-edge background subtraction, then analyzed using least-squares curve-fitting procedures to calculate the structural parameters using theoretically calculated components determined by FEFF3.25 code (14). The parameters with which the FEFF was started were corrected repeatedly until they were identical to the fitting parameters. Bulk Fe_2O_3 and Fe_3O_4 obtained commercially were used as standard samples. A general procedure for the EXAFS analysis has previously been given (5, 7). The parameter error estimates were calculated by the recommended method (15). The correlation between the variables was estimated by the standard method (16).

The best fits to the first peak in the Fe K-edge EXAFS-derived Fourier transform of Fe_3O_4 are summarized in Table 2. Crystal Fe_3O_4 with Fe ions 3/4 in octahedral and 1/4 in tetrahedral interstices will be recognized by EXAFS only in an average sense, i.e., 5.5 oxygens at an average Fe–O distance of 1.97 Å. The fitting parameters indicating 5.8 nearest oxygens in total at an average Fe–O distance of 1.96 Å are in good agreement with the crystal analysis.

3. RESULTS

3.1. Mössbauer Spectra Analyses

Mössbauer spectra of the (a) $Fe/Na–SiO_2$–I, (b) $Fe/Na–SiO_2$–II, and (c) $Na–Fe/SiO_2$ calcined at 800°C are shown in Fig. 2, and the parameters determined by fitting the data are listed in Table 1. From Table 1, it can be concluded according to the IS and QS values that a low-spin Fe^{2+} species is observed on $Fe/Na–SiO_2$–I, while a high-spin Fe^{3+} species is observed on both $Fe/Na–SiO_2$–II and $Na–Fe/SiO_2$.

3.2. XAFS Analysis of Fe/SiO_2

Figure 3 compares the XANES of Fe/SiO_2 with that of bulk Fe_3O_4. It is very common that the high disorder of supported species may significantly blur the XANES. However, the features of Fe/SiO_2, both the intensity of the pre-edge peak and the energy position of the maximum, are very consistent with those of bulk Fe_3O_4, indicating that

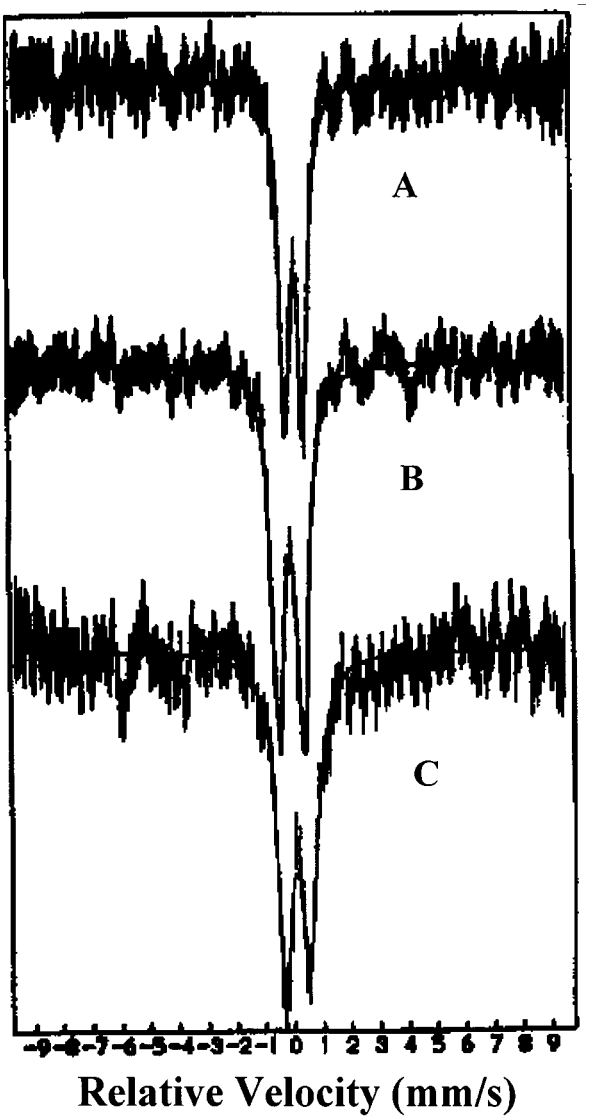

FIG. 2. Mössbauer spectra of (a) Fe/Na–SiO_2–I, (b) Fe/Na–SiO_2–II, and (c) Na–Fe/SiO_2 calcined at 800°C.

the iron ions on the surface of Fe/SiO_2 are present on the sites in a manner very similar to those in Fe_3O_4.

Figure 4 reveals that the calcination temperature has little influence on the site-geometries of the irons on Fe/SiO_2. As the temperature goes up, the XANES spectra of the Fe/SiO_2 calcined at 300, 500, 650, and 800°C (Figs. 4a–d) show no further change in the features. Moreover, the spectral similarities between the catalysts and bulk Fe_3O_4 are well observed. For all four samples, the E_0 revealed by the derivative curves is 13.9 eV and the E_d (the energy difference between the 3d feature and the maximum) is 20.6 eV; both are about 1 eV higher than those of Fe_3O_4.

Figures 5a–d give the Fourier transforms of the Fe/SiO_2 calcined at 300, 500, 650, and 800°C. Generally, Fig. 5a gives a very descriptive understanding of the metal oxides

TABLE 1
Mössbauer Parameters Obtained from the Spectra Shown in Fig. 2

		Fe^{2+}		$Fe Fe^{3+}$	
Sample	Pretreatment	IS (mm/s)	QS (mm/s)	IS (mm/s)	QS (mm/s)
(A) Fe/Na–SiO_2–I	Simply dried at 120°C	0.343	0.641		
(B) Fe/Na–SiO_2–II	Recalcined at 800°C			0.225	0.860
(C) Na–Fe/SiO_2	Calcined at 800°C			0.272	0.846

supported on a substrate surface. Following the most intense peak, there are four or more peaks in the range of 2–5 Å. The most intense peak is contributed to the nearest oxygens, which may come from the surface of silica as well as the external source, i.e., adventitious oxygens. The other peaks in fact reflect all the possible contributions within 5 Å, including not only the nearest irons and the next-nearest oxygens, but also possibly the silicon and adsorbed oxygen molecules. Therefore, the assignments for them are much more complicated in comparison with that of bulk Fe_3O_4. Moreover, they are not well resolved with one another, and the uncertainties in amplitude analysis make the EXAFS fits very difficult. However, in any case, Fig. 5a demonstrates that the dispersion of the irons on Fe/SiO_2 has not been fully reached in its initial stage calcined at 300°C, even though the metal loading would allow it to do so. Further heating improves the dispersion significantly. The contributions from neighbors other than the nearest oxygens are largely suppressed and, in the end, only a weak peak at 2.7 Å (not corrected for phase shift) is left (Fig. 5d). The amplitude

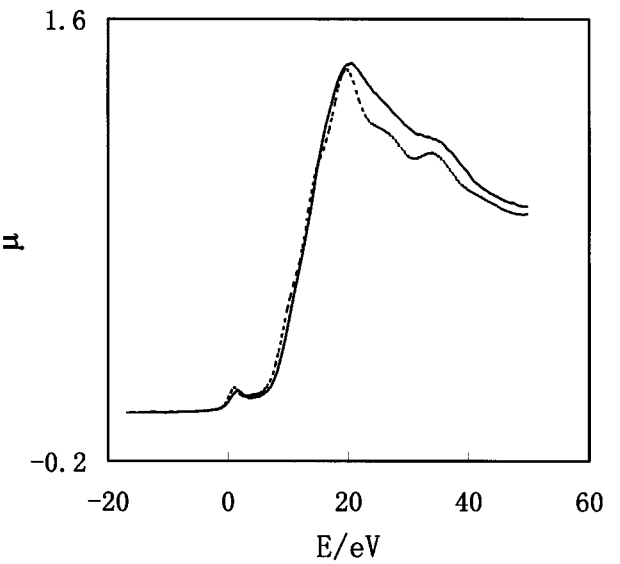

FIG. 3. Fe *K*-edge XANES of Fe/SiO_2 calcined at 800°C and bulk Fe_3O_4 (dashed line).

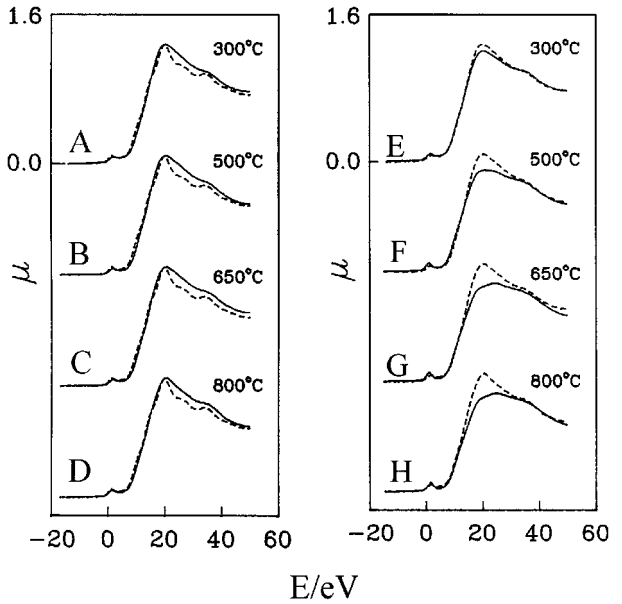

FIG. 4. a–d: Comparison of Fe *K*-edge XANES of Fe/SiO_2 calcined at various temperatures with that of Fe_3O_4 (dashed lines); e–h: Comparison of Fe *K*-edge XANES of $Fe/Na–SiO_2$ calcined at various temperatures with that of Fe/SiO_2 calcined at the same temperature (dashed lines).

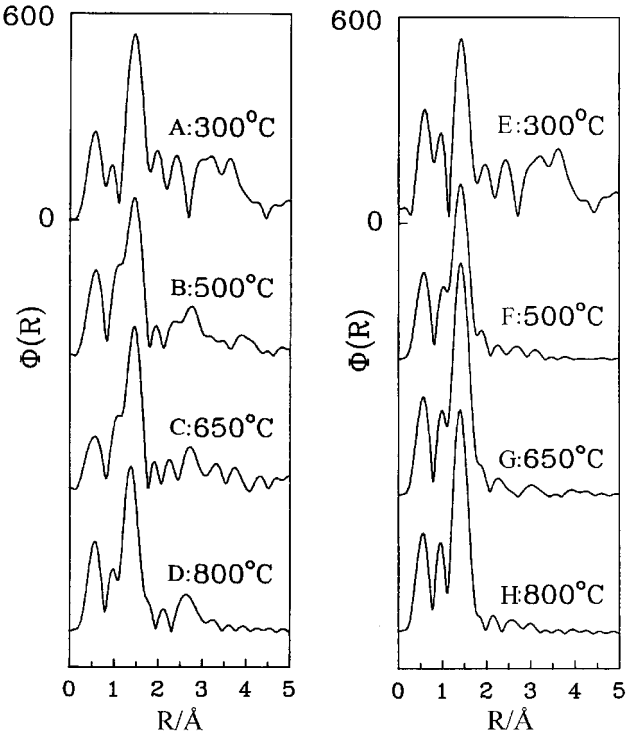

FIG. 5 a–d: Fourier transforms of k^3-weighted EXAFS for Fe/SiO_2 after calcination at various temperatures; e–h: Fourier transforms of the k^3-weighted EXAFS for $Na–Fe/SiO_2$ after calcination at various temperatures.

analysis demonstrates that the nearest irons cause this peak. The best fits to the first peak in the Fourier transform of the Fe/SiO_2 calcined at 800°C and the Fourier-filtered EXAFS therefrom are summarized in Table 2 and Fig. 6. The fits result in 5.0 nearest oxygens for each iron at an average distance of 1.94 Å.

3.3. *XAFS Analysis of Na–Fe/SiO₂*

The XANES spectra of sodium-modified $Na–Fe/SiO_2$ calcined at various temperatures are shown in Figs. 4e–h. It can easily be seen that the $Na–Fe/SiO_2$ after calcination at 300°C does not show any difference from the Fe/SiO_2 calcined at the same temperature. However, after calcination at temperatures higher than 500°C, significant changes in the features are observed. First, intensity of the pre-edge peak is continuously enhanced, from 0.10 (300°C) to 0.12 (500°C), 0.13 (650°C), and finally 0.14 (800°C). The intensity observed for Fe_3O_4 and Fe/SiO_2 is 0.10 and 0.09, respectively. Second, the E_d exhibits a similar trend, i.e., 20.6 eV at 300 and 500°C, but 24.3 eV at 650 and 800°C. And third, the E_0 obtained is 13.9 eV for the sample calcined at 300°C, but only 9.8–10.3 eV for the others.

The Fourier transforms of the $Na–Fe/SiO_2$ calcined at various temperatures are shown in Figs. 5e–h. Although the Fourier transform of the $Na–Fe/SiO_2$ calcined at 300°C (Fig. 5e) shows almost all the peaks observed for $Fe–SiO_2$ treated at the same temperature (Fig. 5a), the samples calcined at higher temperatures obviously exhibit a different picture. The contributions ranging from 2 to 5 Å disappear completely, indicating a highly dispersed character for the catalysts. In comparison with that of the Fe/SiO_2 calcined at 800°C, the intensity of the most intense peak for the $Na–Fe/SiO_2$ calcined at 800°C (Fig. 5h) is markedly enhanced, growing about 1/4 in relative height and indicating a more closely spaced oxygen shell for the irons. The best fits to this peak and the Fourier-filtered EXAFS therefrom are summarized in Fig. 6 and Table 2. A total of 4.1 nearest oxygens is found for each iron site at a remarkably shortened distance of 1.89 Å.

3.4. *XAFS Analysis of Fe/Na–SiO₂*

There are clearly two possibilities for the formation of the tetrahedral sites in the presence of a sodium promoter. One is that the sodium promoter reacts with the silica to provide the cristobalite exposed faces, which would favor a predominant tetrahedral phase for the deposition of iron ions. The second is that the sodium promoter helps the iron ions move to the tetrahedral sites of silica under higher-temperature heating, whether or not the reconstruction of the silica would occur.

Two $Fe/Na–SiO_2$ samples were therefore prepared and investigated. The $Fe/Na–SiO_2$–I, which was obtained by

TABLE 2
EXAFS-Derived Coordination Number (CN), Shell Radius (R), and Debye-Waller Factors (D–W, $\Delta\sigma^2$)

Sample	Shell	CN	R (Å)	D–W ($Å^{-1}$)	R–factor	Filtering range
Fe_3O_4	Fe–O	5.8	1.97	0.010	0.10	0.76–1.93 Å
Fe/SiO_2	Fe–O	5.0	1.94	0.005	0.14	0.76–1.94 Å
$Fe/Na–SiO_2–I^a$	Fe–O	5.5	1.94	0.005	0.12	0.76–1.98 Å
$Fe/Na–SiO_2–II^a$	Fe–O	4.1	1.89	0.002	0.14	0.76–1.97 Å
$Na–Fe/SiO_2^a$	Fe–O	4.7	1.88	0.002	0.14	0.76–1.97 Å

Note. Fitting range in k-space: 1.5–12.6 $Å^{-1}$ with the weight of k^3.
[a]The same catalysts as shown in Table. 1

depositing the irons on sodium-induced reconstructed silica without high-temperature recalcination, shows XANES features (Fig. 7a) the same as that of Fe/SiO_2 (Fig. 3), indicating that the irons are not dominated by a tetrahedral phase without further calcination, although the reconstructed silica surface would allow them to be. However, after recalcination at 800°C, the $Fe/Na–SiO_2$–II retains all the spectral features of the $Fe/Na–SiO_2$ (800°C), as shown in Fig. 7b. The EXAFS-derived Fourier transforms shown in Fig. 8 exhibit a similar trend. It can be found that the transform of $Fe/Na–SiO_2$–I is very similar to that of the Fe/SiO_2 calcined at 800°C, e.g., behind the most intense peak caused by the nearest oxygens, follows a fairly intense, independent peak (together with an observable shoulder) rising from the nearest iron contributions. However, the transform of $Fe/Na–SiO_2$–II is the same as that of the $Na–Fe/SiO_2$ calcined at 800°C: behind the most intense peak, no further contribution can be seen. The best fits to the most intense peaks for the two samples are summarized in Fig. 9 and Table 2. Mössbauer spectrum analysis has shown that the irons on the $Na–Fe/SiO_2$ (800°C) and the $Fe/Na–SiO_2$–II are high-spin Fe^{3+} species. It can be seen from Tables 1 and 2 that the spectral similarities observed between Fe/SiO_2 and $Fe/Na–SiO_2$–I, and between $Na–Fe/SiO_2$ and $Fe/Na–SiO_2$–II, are fully supported by the structural parameters obtained in details.

It is noteworthy that the XANES spectra of the $Na–Fe/SiO_2$ and $Fe/Na–SiO_2$, both calcined at 800°C, are virtually identical to that reported for the tetrahedrally coordinated Fe^{3+} ions in iron-containing silicate glass (17), as shown in Fig. 10.

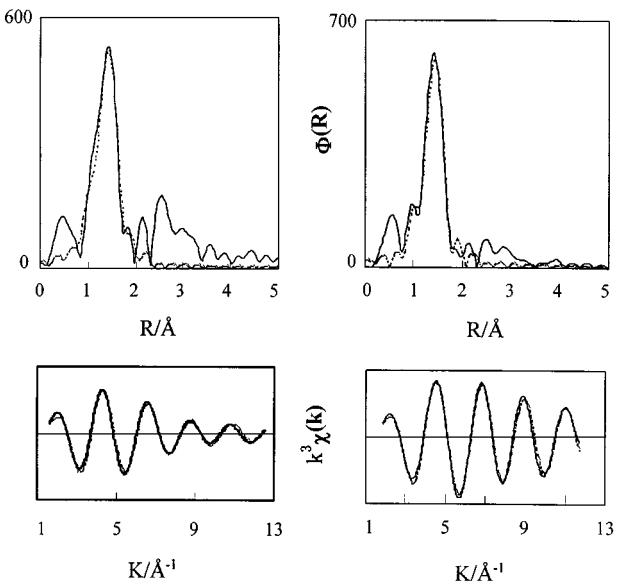

FIG. 6. The best fits to the first peak in the Fourier transform and the filtered EXAFS therefrom for the Fe/SiO_2 calcined at 800°C (left) and the $Na–Fe/SiO_2$ calcined at 800°C (right).

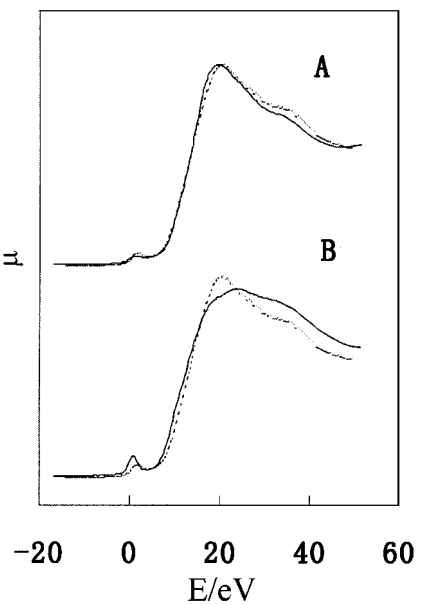

FIG. 7. Comparison of Fe K-edge XANES of (a) $Fe/Na–SiO_2$–I and (b) $Fe/Na–SiO_2$–II with that of Fe_3O_4 (dashed lines).

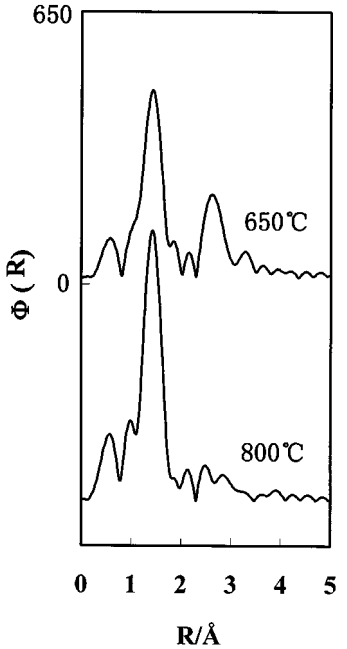

FIG. 8. Fourier transforms of the k^3-weighted EXAFS for Fe/Na–SiO_2–I and –II.

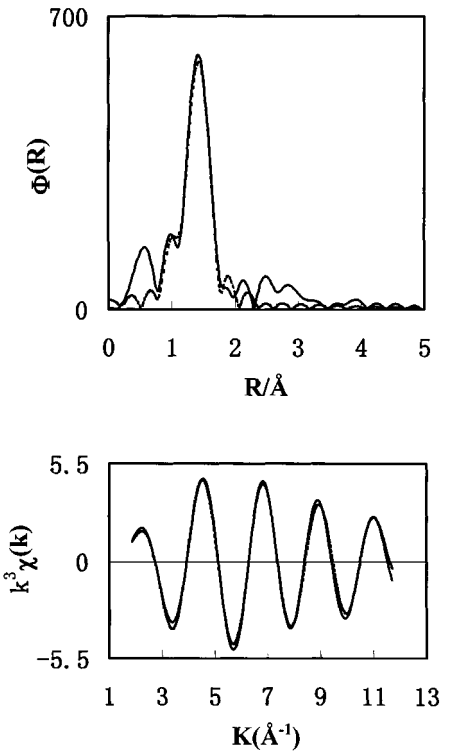

FIG. 9. The best fits to the first peak in the Fourier transform and the filtered EXAFS of Fe/Na–SiO_2–II.

4. DISCUSSION

Clearly, the XANES and EXAFS results described above dipict the migration/dispersion of iron cations on the support surface. With or without the participation of a sodium promoter, two different processes have been observed.

The unmodified Fe/SiO_2 gives a general understanding of the dispersion. The iron cations deposited on the surface at its first stage, e.g., calcined at 300°C, are randomly distributed. There is a series of neighbors in the range 2–5 Å, as indicated by the Fourier transforms. The dispersion of the irons monitored by the transforms is progressively improved as the temperature increases. However, XANES spectra show that regarding the site-geometries of the irons the surface species is similar to bulk Fe_3O_4 and not different from after treatment at various temperatures. The fact that no change is found in the site-symmetries of the irons implies that the dispersion process is achieved by heating pretreatment, probably through replacement of the oxygens in small Fe_3O_4 particles by the oxygens of silica, i.e., Fe–O–Si linkages are formed through the process.

The participation of sodium changes the environment. Originally, the Na–Fe/SiO_2 calcined at 300°C shows the same XANES and EXAFS spectra as those observed for Fe/SiO_2, revealing that both have the same starting structures at 300°C. However, in the presence of sodium, higher-temperature treatment converts these predominantly octahedral iron sites to tetrahedral coordination in a step-by-step mode, demonstrated by a steadily increased pre-edge peak, a continuously increased E_d, and a gradually enhanced backscattering of the nearest oxygens. Finally, only a tetrahedral ferric iron phase remains on the surface.

5. CONCLUSIONS

1. The dispersion of iron oxides on silica depends significantly on the calcinating temperatures. A calcination

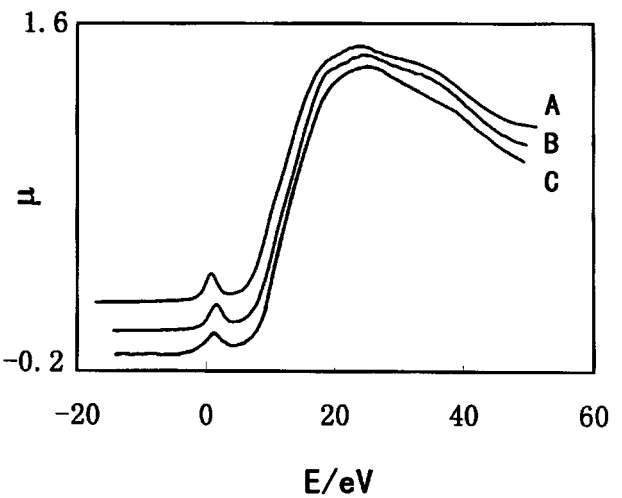

FIG. 10. Comparison of Fe *K*-edge XANES of (a) Fe/Na–SiO_2–II and (b) Na–Fe/SiO_2 calcined at 800°C with (c) tetrahedrally coordinated Fe^{3+} irons in iron-containing silicate glass.

temperature higher than 650°C is needed to reach greater dispersion.

2. Migration of irons on Fe/SiO_2 has been observed. The migration shows limited influence on the iron site-geometries, but results in a better dispersion for the irons after calcination at higher temperatures.

3. A sodium promoter plays an important role in converting predominantly octahedral irons into tetrahedral coordination. Comparative studies on $Fe/Na–SiO_2$ and $Na–Fe/SiO_2$ suggest that the function of the sodium promoter is achieved at about 800°C by simultaneous transformation of the amorphous silica to α-cristobalite, which can provide many more tetrahedral sites for the irons moving through calcination.

ACKNOWLEDGMENTS

The project was supported by the National Natural Science Foundation, China. We are grateful to the Photon Factory for the use of BL-7L facilities. We thank Professor M. Nomura for experimental assistance.

REFERENCES

1. V. E. Henrich and P. A. Cox, "Surface Sciences of Metal Oxides." Cambridge University Press, New York, 1996.
2. D. G. Rethwisch and J. A. Dumesic, *J. Phys. Chem.* **90,** 1863 (1986).
3. H. Hu, I. E. Wachs, and S. R. Bare, *J. Phys. Chem.* **99,** 10897 (1995).
4. H. Hu and I. E. Wachs, *J. Phys. Chem.* **99,** 10911 (1995).
5. Y. Kou, Z.-H. Suo, and H.-L. Wang, *J. Catal.* **149,** 246 (1994).
6. Y. Kou, H.-L. Wang, J.-Z. Niu, and W.-J. Ji, *J. Phys. Chem.* **100,** 2330 (1996).
7. Y. Kou, H.-L. Wang, M. Te, T. Tanaka, and M. Nomura, *J. Catal.* **141,** 660 (1993).
8. Y. Kou, Z.-H. Suo, J.-Z. Niu, W.-Z. Zhang, and H.-L. Wang, *Catal. Lett*. **35,** 271 (1995).
9. Y. Kou, Z.-H. Suo, J.-Z. Niu, W.-Z. Zhang, and H.-L. Wang, *Catal. Lett*. **35,** 279 (1995).
10. F. A. Cotton and G. Wilkinson, "Advanced Inorganic Chemistry," p. 386. Wiley, New York, 1980.
11. C. A. Jones, J. J. Leonard, and J. A. Sofranko, *J. Catal.* **103,** 311 (1987).
12. A. Machocki, A. Denis, T. Borowiecki, and J. Barcicki, *Appl. Catal.* **72,** 283 (1991).
13. D. Wang, M. P. Rosynek, and J. H. Lunsford, *J. Catal.* **155,** 390 (1995).
14. J. Rehr, J. Mustre de Leon, S. I. Zabinsky, and R. C. Albers, *J. Am. Chem. Soc*. **113,** 5135 (1991).
15. F. W. Lytle, D. E. Sayers, and E. A. Stern, *Physica B* **158,** 701 (1989).
16. A. D. Cox, *in* "EXAFS for Inorganic Systems." DL/SCI/R17, Daresbury, 1981.
17. A. Bianconi, E. Fritsch, G. Calas, and J. Peliau, *Phys. Rev. B* **32,** 4292 (1985).